Quantum Monte Carlo calculations for light nuclei using chiral forces

Joel Lynn

Theoretical Division, Los Alamos National Laboratory

March 19, 2014

Outline

Motivation

Ab-initio calculations for nuclei - Quantum Monte Carlo (QMC)

- Nuclear structure methods seek to solve the many-body Schrödinger equation

$$H\left|\Psi\right\rangle = E\left|\Psi\right\rangle .$$

- Variational Monte Carlo (VMC) uses a Metropolis random walk to calculate an upper bound to the ground-state energy:

$$E_T = \frac{\langle \Psi_T | H | \Psi_T \rangle}{\langle \Psi_T | \Psi_T \rangle} \geq E_0.$$

- Green's function Monte Carlo (GFMC) uses propagation in imaginary time to project out the ground state.

$$\left|\Psi(\tau)\right\rangle = e^{-H\tau}\left|\Psi_T\right\rangle \Rightarrow \lim_{\tau\to\infty}\left|\Psi(\tau)\right\rangle \propto \left|\Psi_0\right\rangle .$$

Motivation

Ab-initio calculations for nuclei - QMC

GFMC enjoys a reputation as the most accurate method for solving the many-body Schrödinger equation for light nuclei $4 < A \leq 12$.

- First: VMC.
  - We begin with a trial wave function Ψ_T and generate a random position: $\mathbf{R} = \mathbf{r}_1, \mathbf{r}_2, \ldots, \mathbf{r}_A$.
  - Use the Metropolis algorithm to generate new positions $\mathbf{R}'$ based on the probability $P = \frac{|\Psi_T(\mathbf{R}')|^2}{|\Psi_T(\mathbf{R})|^2}$.
  - This gives us a set of "walkers" distributed according to the trial wave function: $\sum_\beta c_\beta |\mathbf{R}\beta\rangle$. $3A$ positions and $2^A \binom{A}{Z}$ spin/isospin states in the charge basis.

Motivation

Ab-initio calculations for nuclei - QMC

- Second: GFMC.
  - The wave function is imperfect: $\Psi_T = \Psi_0 + \sum_{i \neq 0} c_i \Psi_i$.
  - Propagate in imaginary time to project out the ground state Ψ_0:

$$\Psi(\tau) = e^{-(H-E_T)\tau}\Psi_T = e^{-(E_0-E_T)\tau}\left[\Psi_0 + \sum_{i\neq 0} c_i e^{-(E_i-E_0)\tau}\Psi_i\right]$$

$$\Rightarrow \lim_{\tau\to\infty} \Psi(\tau) \propto \Psi_0.$$

Motivation

Ab-initio calculations for nuclei - QMC

- Second: GFMC.
  The Green's function is calculated by introducing the short-imaginary time $\Delta\tau = \tau/n$.

$$\Psi(\tau) = [\underbrace{e^{-(H-E_T)\Delta\tau}}_{G_{\alpha\beta}(\mathbf{R},\mathbf{R}';\Delta\tau)}]^n \Psi_T$$

$$G_{\alpha\beta}(\mathbf{R},\mathbf{R}';\Delta\tau) = \langle \mathbf{R}\alpha | e^{-(H-E_T)\Delta\tau} | \mathbf{R}'\beta \rangle$$

$$\Psi(\mathbf{R}_n,\tau) = \int d\boldsymbol{\mathcal{R}} G(\mathbf{R}_n,\mathbf{R}_{n-1}) \cdots G(\mathbf{R}_1,\mathbf{R}_0)\Psi_T(\mathbf{R}_0)$$

$$d\boldsymbol{\mathcal{R}} = \prod_{i=0}^{n-1} d\mathbf{R}_i$$

Motivation

Ab-initio calculations for nuclei - QMC

- Second: GFMC.
  - We can calculate so-called "mixed estimates":

$$\frac{\langle \Psi(\tau)|O|\Psi_T\rangle}{\langle \Psi(\tau)|\Psi_T\rangle} = \frac{\int d\boldsymbol{\mathcal{R}} \Psi_T^\dagger(\mathbf{R}_n) G^\dagger(\mathbf{R}_n, \mathbf{R}_{n-1}) \cdots G^\dagger(\mathbf{R}_1, \mathbf{R}_0) O \Psi_T(\mathbf{R}_0)}{\int d\boldsymbol{\mathcal{R}} \Psi_T^\dagger(\mathbf{R}_n) G^\dagger(\mathbf{R}_n, \mathbf{R}_{n-1}) \cdots G^\dagger(\mathbf{R}_1, \mathbf{R}_0) \Psi_T(\mathbf{R}_0)}.$$

$$\langle O(\tau)\rangle = \frac{\langle \Psi(\tau)|O|\Psi(\tau)\rangle}{\langle \Psi(\tau)|\Psi(\tau)\rangle} \approx \langle O(\tau)\rangle_{\text{Mixed}} + [\langle O(\tau)\rangle_{\text{Mixed}} - \langle O\rangle_T].$$

  - For ground-state energies, $O = H$, and $[H, G] = 0$:

$$\langle H\rangle_{\text{Mixed}} = \frac{\langle \Psi_T|e^{-(H-E_T)\tau/2} H e^{-(H-E_T)\tau/2}|\Psi_T\rangle}{\langle \Psi_T|e^{-(H-E_T)\tau/2} e^{-(H-E_T)\tau/2}|\Psi_T\rangle}$$

$$\lim_{\tau\to\infty} \langle H\rangle_{\text{Mixed}} = E_0.$$

Motivation

Nuclear interactions - Nucleons

- A fundamental goal of low-energy nuclear physics is to describe and calculate properties of nuclei in terms of realistic bare nuclear interactions.
- Quantum chromodynamics (QCD) is the underlying theory, but nucleons are the relevant degrees of freedom for low-energy nuclear physics $\rightarrow$ nucleon-nucleon potentials.

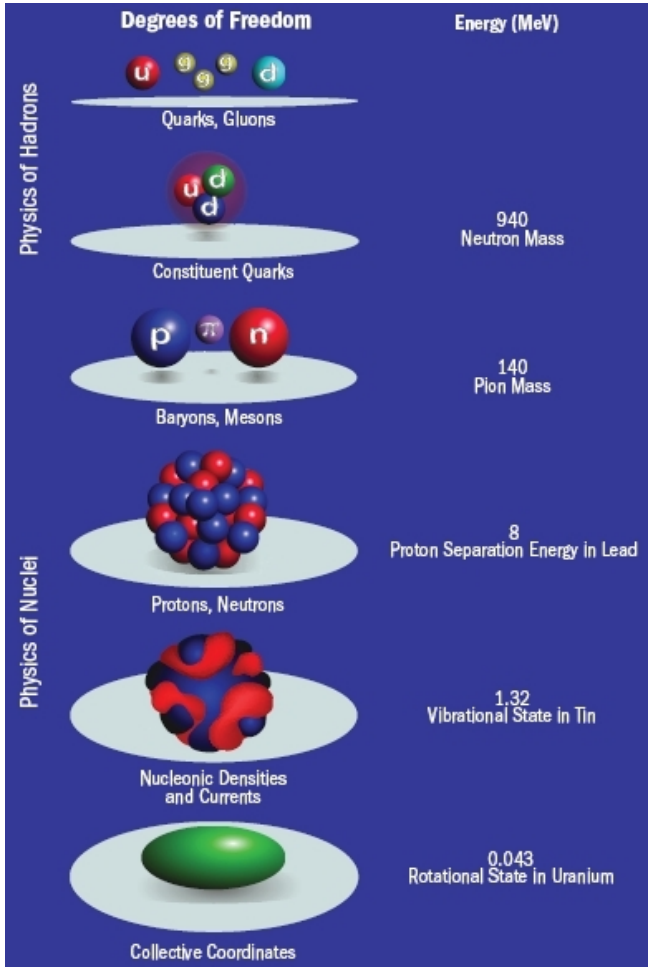

Figure 1: From www.scidacreview.org

Motivation

Nuclear interactions - The Hamiltonian

$$H = \sum_{i=1}^{A} \frac{\mathbf{p}_i^2}{2m_i} + \sum_{i<j}^{A} v_{ij} + \sum_{i<j<k}^{A} V_{ijk} + \cdots$$

The focus of this talk is on the two-body interaction. Until now, there were two broad choices for v_{ij}.

- Local, real-space, phenomenological: Argonne's v_{18}[1] - informed by theory, phenomenology, and experiment (well tested and very successful).
- Non-local, momentum-space, effective field theory (EFT): N^{3}LO[2] - informed by chiral EFT and experiment (well liked and often used in basis-set methods, such as the no-core shell model).

[1] R. B. Wiringa, V. G. J. Stoks, and R. Schiavilla, Phys. Rev. C **51**, 38 (1995).

[2] e.g. D. R. Entem and R. Machleidt, Phys. Rev. C **68**, 041001 (2003)

Motivation

Nuclear interactions - Argonne's v_{18}

Argonne's v_{18} consists of three parts.

$$v_{ij} = v_{ij}^{\gamma} + v_{ij}^{\pi} + v_{ij}^{R}.$$

- v_{ij}^{γ} includes one- and two-photon exchange Coulomb interactions, vacuum polarization, Darwin-Foldy, and magnetic moment terms with appropriate proton and neutron form factors.
- v_{ij}^{π} includes charge-dependent terms due to the difference in neutral and charged pion masses.
- v_{ij}^{R} is a short-range phenomenological potential.

Motivation

Nuclear interactions - Argonne's v_{18}

Operator form

$$v_{ij}^{\pi} + v_{ij}^{R} = \sum_{p=1}^{18} v_p(r_{ij})\, O_{ij}^{p}.$$

Charge-independent operators

$$O_{ij}^{p=1,14} = \left[1, \boldsymbol{\sigma}_i \cdot \boldsymbol{\sigma}_j, S_{ij}, \mathbf{L}\cdot\mathbf{S}, \mathbf{L}^2, \mathbf{L}^2(\boldsymbol{\sigma}_i \cdot \boldsymbol{\sigma}_j), (\mathbf{L}\cdot\mathbf{S})^2\right] \otimes \left[1, \boldsymbol{\tau}_i \cdot \boldsymbol{\tau}_j\right].$$

Charge-independence-breaking operators

$$O_{ij}^{p=15,18} = [1, \boldsymbol{\sigma}_i \cdot \boldsymbol{\sigma}_j, S_{ij}] \otimes T_{ij}, \text{ and } (\tau_{zi} + \tau_{zj}).$$

Tensor operators

$$S_{ij} = 3(\boldsymbol{\sigma}_i \cdot \hat{\mathbf{r}}_{ij})(\boldsymbol{\sigma}_j \cdot \hat{\mathbf{r}}_{ij}) - \boldsymbol{\sigma}_i \cdot \boldsymbol{\sigma}_j,\ T_{ij} = 3\tau_{zi}\tau_{zj} - \boldsymbol{\tau}_i \cdot \boldsymbol{\tau}_j$$

Motivation

Nuclear interactions - Argonne's v_{18}

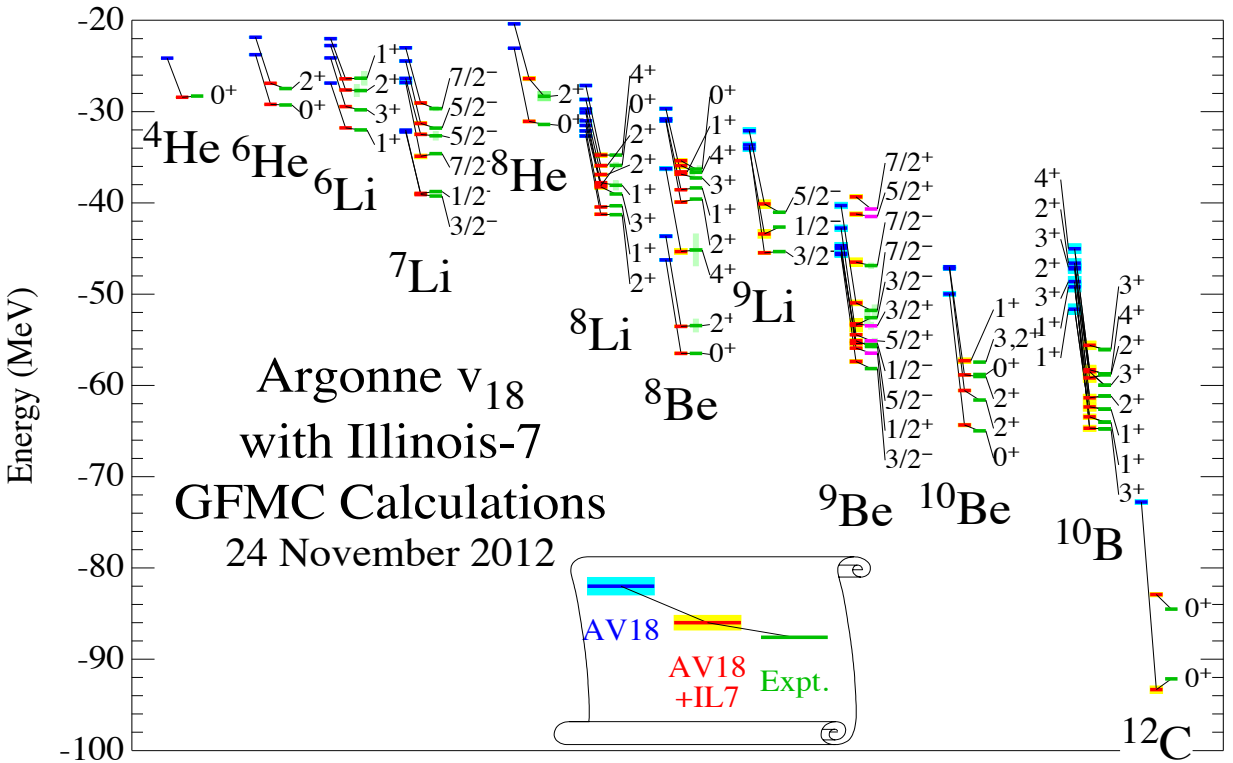

Figure 2: Many excellent results using Green's function Monte Carlo (GFMC) and phenomenological potentials. From http://www.phy.anl.gov/theory.

This is great! But... Until now the nucleon-nucleon potentials used have been restricted to the phenomenological Argonne-Urbana/Illinois family of interactions.

Motivation

Nuclear interactions - Chiral EFT

Chiral EFT makes a more direct connection between QCD and the nuclear force.

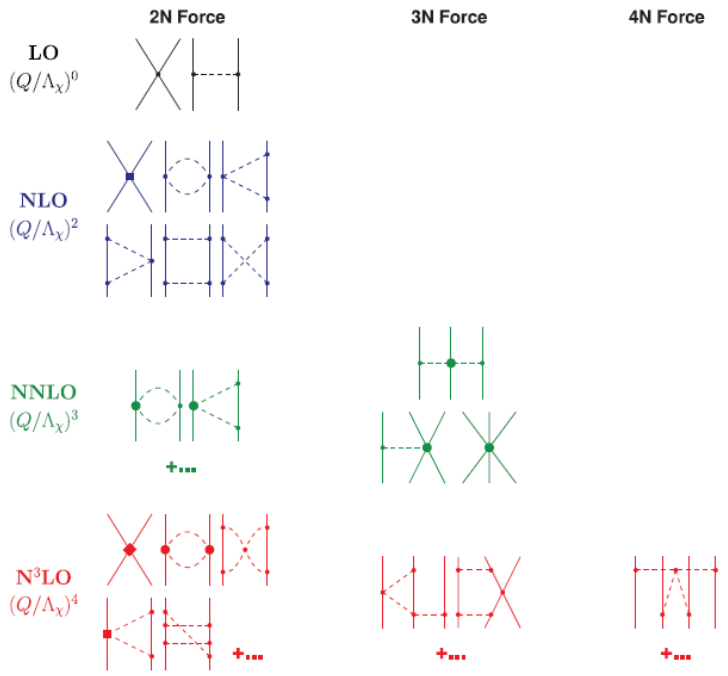

Figure 3: Hierarchy of the nuclear force in chiral EFT, from R. Machleidt and D. Entem, Phys. Rep. **503**, 1 (2011).

Weinberg prescription

- Start from the most general Lagrangian consistent with all symmetries of the underlying interaction...
  $\mathcal{L} = \mathcal{L}_{\pi\pi} + \mathcal{L}_{\pi N} + \mathcal{L}_{NN} + \cdots$
- Define a power-counting scheme...
  $\nu = -4 + 2N + 2L + \sum_i V_i \Delta_i,$
  $\Delta_i = d_i + \frac{1}{2} n_i - 2.$

Motivation

Nuclear interactions - Chiral EFT

Chiral EFT makes a more direct connection between QCD and the nuclear force.

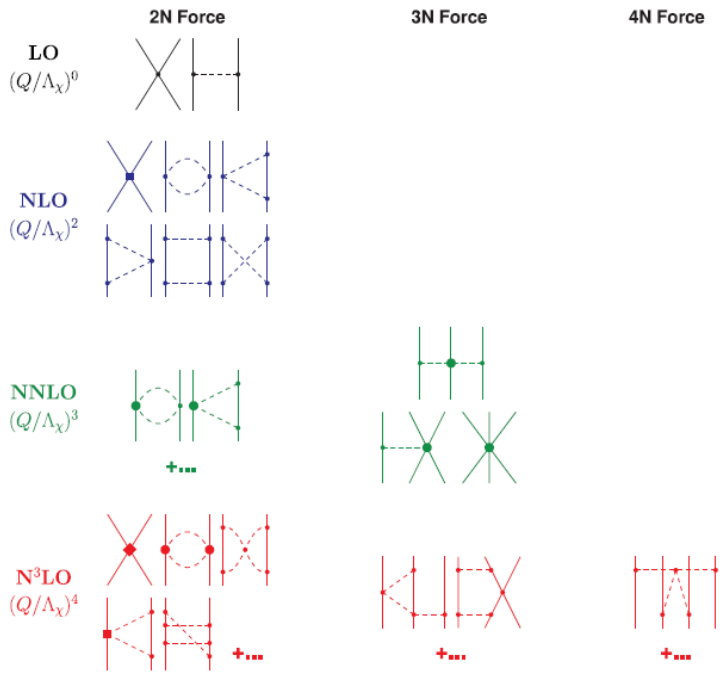

Figure 3: Hierarchy of the nuclear force in chiral EFT, from R. Machleidt and D. Entem, Phys. Rep. **503**, 1 (2011).

Weinberg prescription

- An expansion in (Q/Λ_χ).
- Q is a soft momentum scale.
- $\Lambda_\chi \sim 1$ GeV is the chiral-symmetry-breaking scale.

For example, the leading-order (LO) diagrams lead to

$$V_{NN}^{(0)} \propto \frac{(\boldsymbol{\sigma}_1 \cdot \mathbf{q})(\boldsymbol{\sigma}_2 \cdot \mathbf{q})}{\mathbf{q}^2 + M_\pi^2} \boldsymbol{\tau}_1 \cdot \boldsymbol{\tau}_2 + \cdots$$

Motivation

Nuclear interactions - Chiral EFT

Chiral EFT makes a more direct connection between QCD and the nuclear force.

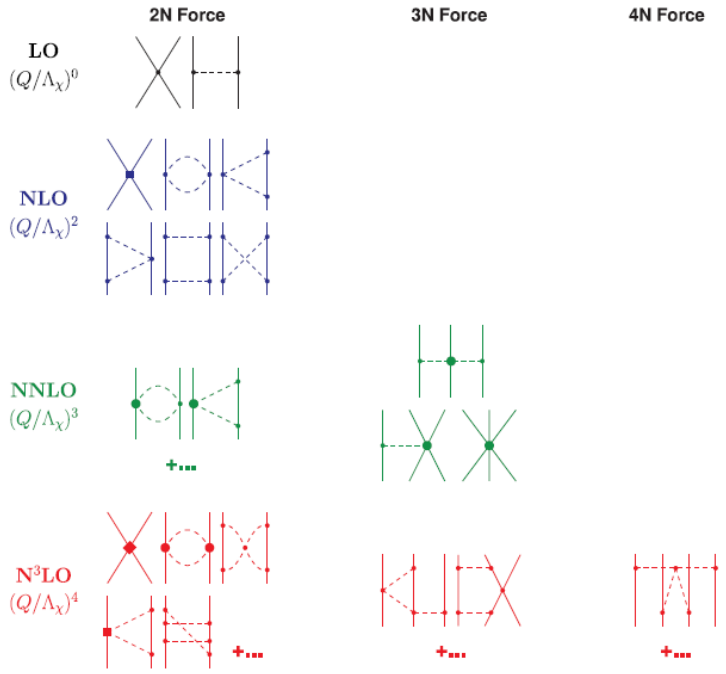

Figure 3: Hierarchy of the nuclear force in chiral EFT, from R. Machleidt and D. Entem, Phys. Rep. **503**, 1 (2011).

Sources of non-locality in standard approach[a] [b]

- Regulator:
  $f(p,p') = e^{-(p/\Lambda)^n} e^{-(p'/\Lambda)^n}$.
- Contact interactions
  $\propto \mathbf{k} = (\mathbf{p}+\mathbf{p}')/2$.

$\mathcal{F}[V(\mathbf{p},\mathbf{p}')] \rightarrow V(\mathbf{r},\mathbf{r}')$.

---

[a] D. Entem and R. Machleidt, Phys. Rev. C **68**, 041001 (2003)

[b] E. Epelbaum, W.Glöckle and U.-G. Meißner, Eur. Phys. J. A **19**, 401 (2004)

Motivation

Nuclear interactions - Chiral EFT

Chiral EFT makes a more direct connection between QCD and the nuclear force.

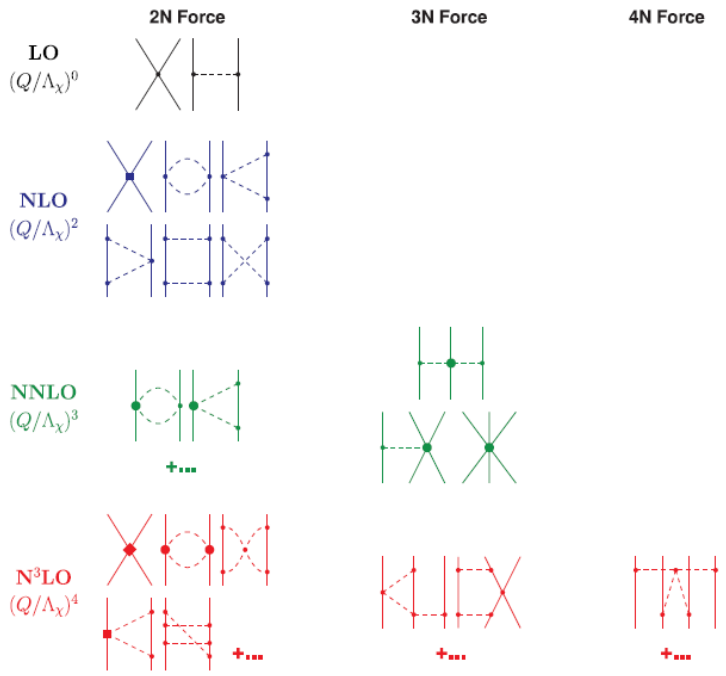

Figure 3: Hierarchy of the nuclear force in chiral EFT, from R. Machleidt and D. Entem, Phys. Rep. **503**, 1 (2011).

New approach[a]

- Regulator: $f_{\text{long}}(r) = 1 - e^{-(r/R_0)^4}$.
- Up to N^{2}LO, $V_\pi = V_\pi(\mathbf{q})$, $\mathbf{q} = \mathbf{p}' - \mathbf{p}$.

$\mathcal{F}[V(\mathbf{q})] \rightarrow V(\mathbf{r})$

$\Rightarrow$ Local!

---

[a] A. Gezerlis et al., Phys. Rev. Lett. **111**, 032501 (2013)

Motivation

Nuclear interactions - Chiral EFT

Chiral EFT makes a more direct connection between QCD and the nuclear force.

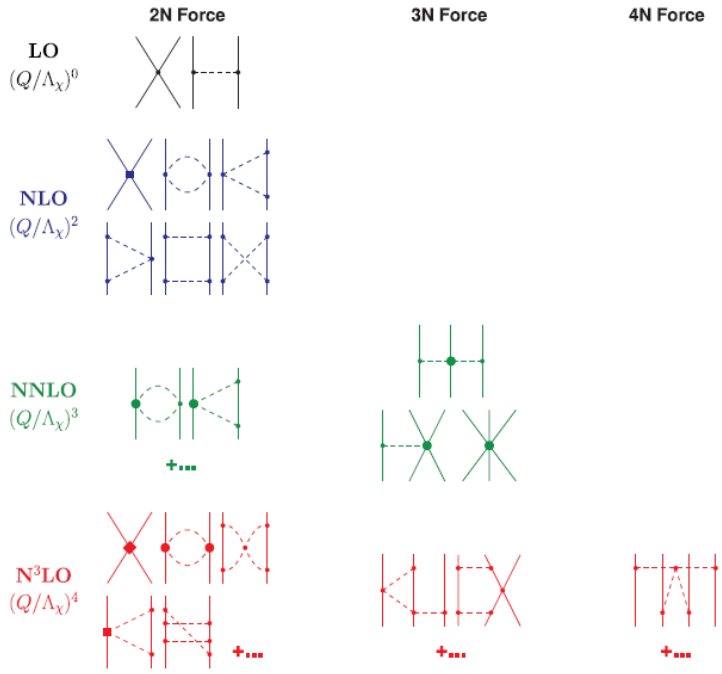

Figure 3: Hierarchy of the nuclear force in chiral EFT, from R. Machleidt and D. Entem, Phys. Rep. **503**, 1 (2011).

New approach[a]

$$V(r) = V_C(r) + W_C(r)\boldsymbol{\tau}_1 \cdot \boldsymbol{\tau}_2 + (V_S(r) + W_S(r)\boldsymbol{\tau}_1 \cdot \boldsymbol{\tau}_2)\boldsymbol{\sigma}_1 \cdot \boldsymbol{\sigma}_2 + (V_T(r) + W_T(r)\boldsymbol{\tau}_1 \cdot \boldsymbol{\tau}_2)S_{12}.$$

$$V_C(r) = \frac{1}{2\pi^2 r}\int_{2M_\pi}^{\tilde{\Lambda}} d\mu \mu e^{-\mu r}\rho_C(\mu), \text{ etc.}$$

[a] A. Gezerlis et al., Phys. Rev. Lett. **111**, 032501 (2013)

Motivation

Nuclear interactions - Chiral EFT

Local chiral EFT potential $\sim$ a v_7 potential

$$v_{ij} = \sum_{p=1}^{7} v_p(r_{ij})\, O_{ij}^{p} + \sum_{p=15}^{18} v_p(r_{ij})\, O_{ij}^{p}.$$

Charge-independent operators

$$O_{ij}^{p=1,14} = \left[1, \boldsymbol{\sigma}_i \cdot \boldsymbol{\sigma}_j, S_{ij}, \mathbf{L}\cdot\mathbf{S}, \mathbf{L}^2, \mathbf{L}^2(\boldsymbol{\sigma}_i \cdot \boldsymbol{\sigma}_j), (\mathbf{L}\cdot\mathbf{S})^2\right] \otimes \left[1, \boldsymbol{\tau}_i \cdot \boldsymbol{\tau}_j\right].$$

Charge-independence-breaking operators

$$O_{ij}^{p=15,18} = [1, \boldsymbol{\sigma}_i \cdot \boldsymbol{\sigma}_j, S_{ij}] \otimes T_{ij}, \text{ and } (\tau_{zi} + \tau_{zj}).$$

Tensor operators

$$S_{ij} = 3(\boldsymbol{\sigma}_i \cdot \hat{\mathbf{r}}_{ij})(\boldsymbol{\sigma}_j \cdot \hat{\mathbf{r}}_{ij}) - \boldsymbol{\sigma}_i \cdot \boldsymbol{\sigma}_j, \; T_{ij} = 3\tau_{zi}\tau_{zj} - \boldsymbol{\tau}_i \cdot \boldsymbol{\tau}_j$$

Motivation

Nuclear interactions - Chiral EFT

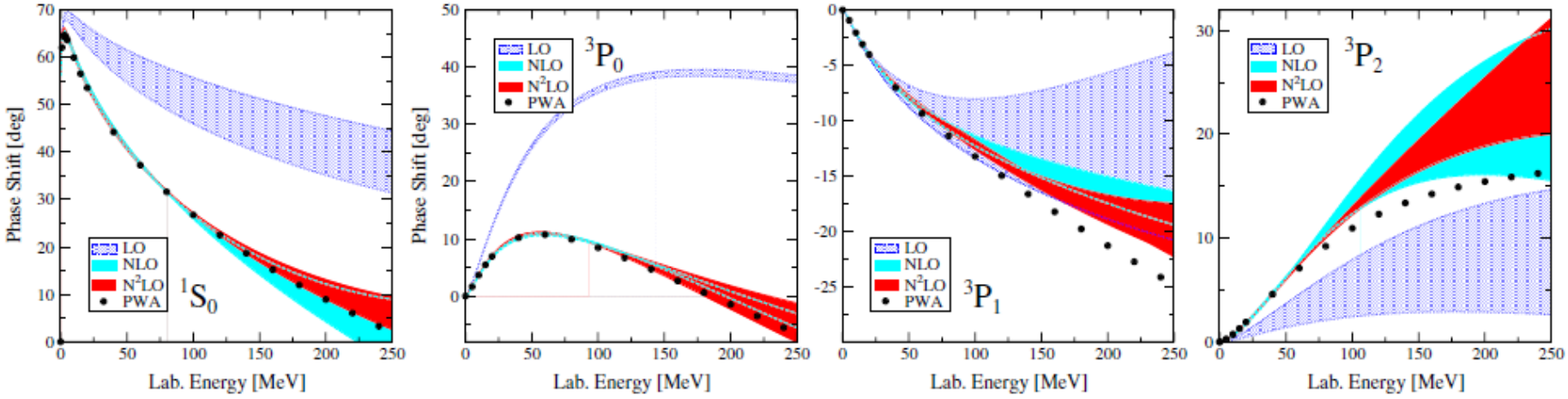

Figure 4: Phase shifts for the *np* potential. From A. Gezerlis et al., Phys. Rev. Lett. **111**, 032501 (2013)

Motivation

Nuclear interactions - Chiral EFT

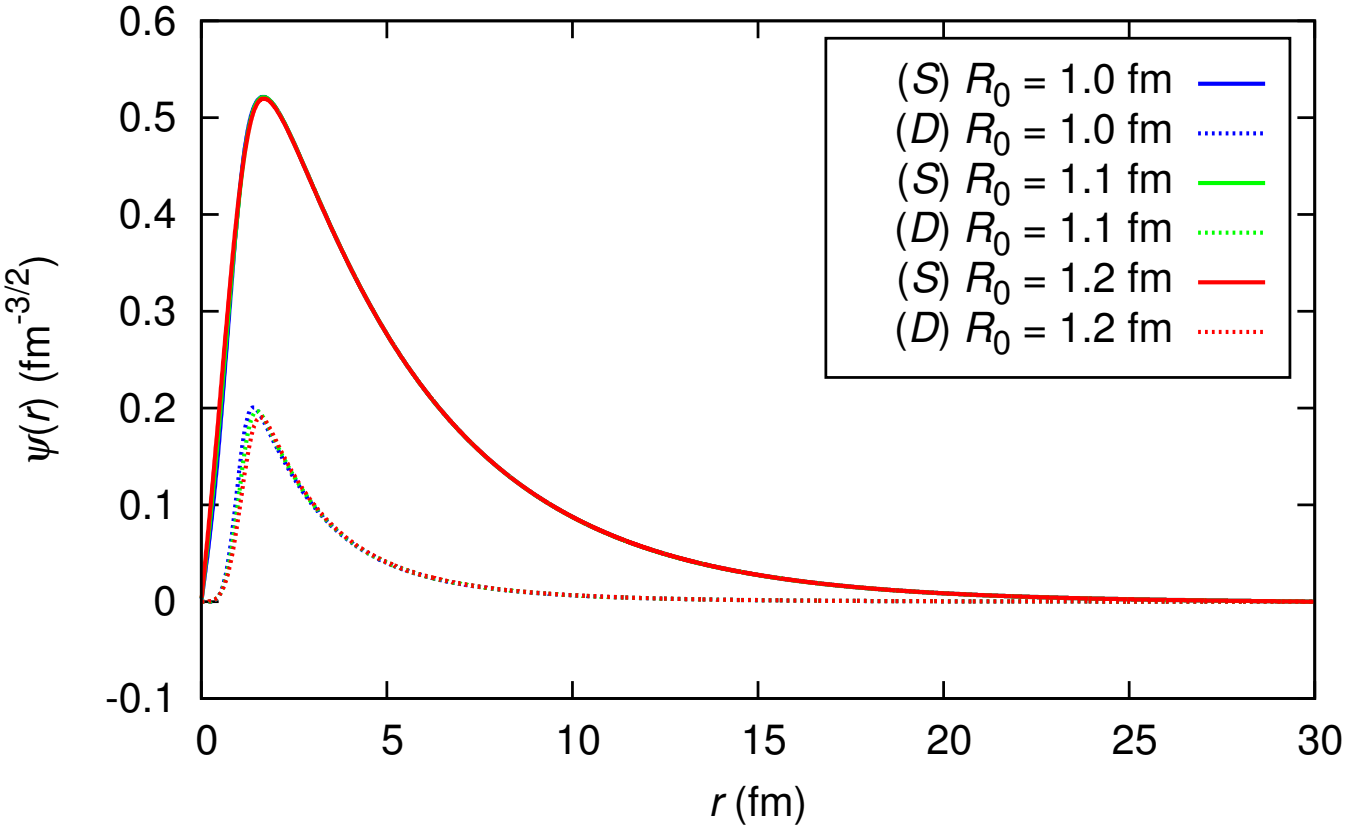

Figure 5: Deuteron wave functions at N^2LO.

Results

^{2}H binding energies - $\langle H \rangle$

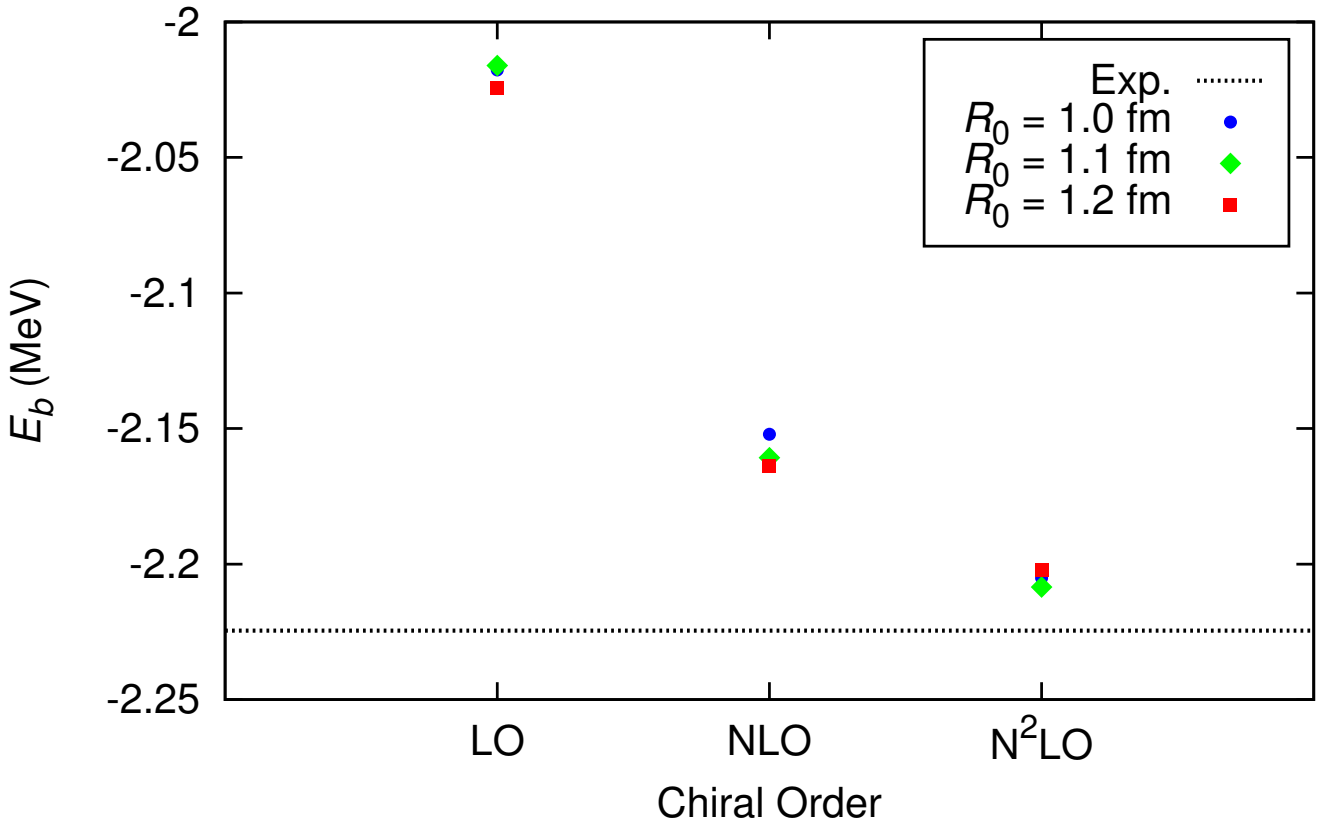

Figure 6: ^{2}H binding energy at different chiral orders and cutoff values.

Results

^{3}H binding energies - $\langle H \rangle$

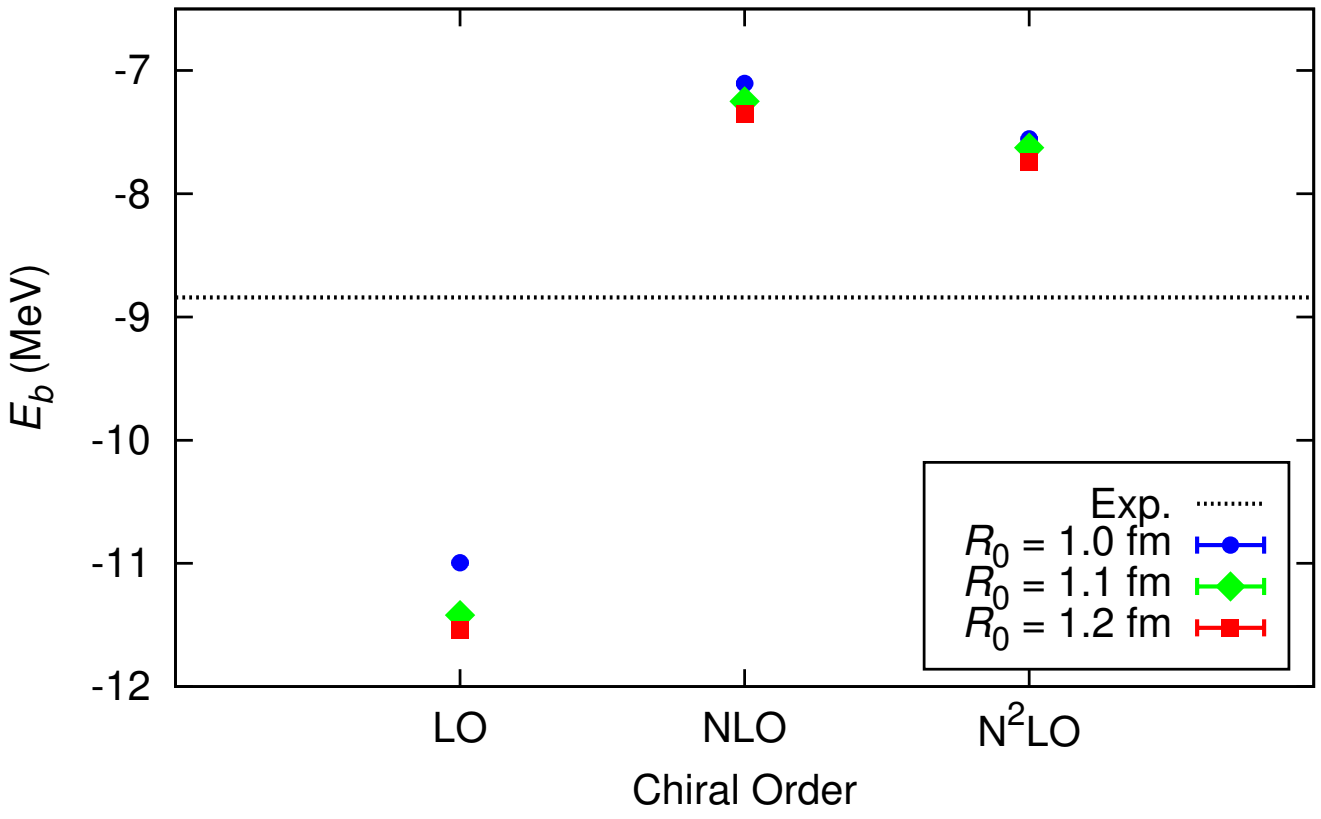

Figure 7: ^{3}H binding energy at different chiral orders and cutoff values.

Results

^{3}He binding energies - $\langle H \rangle$

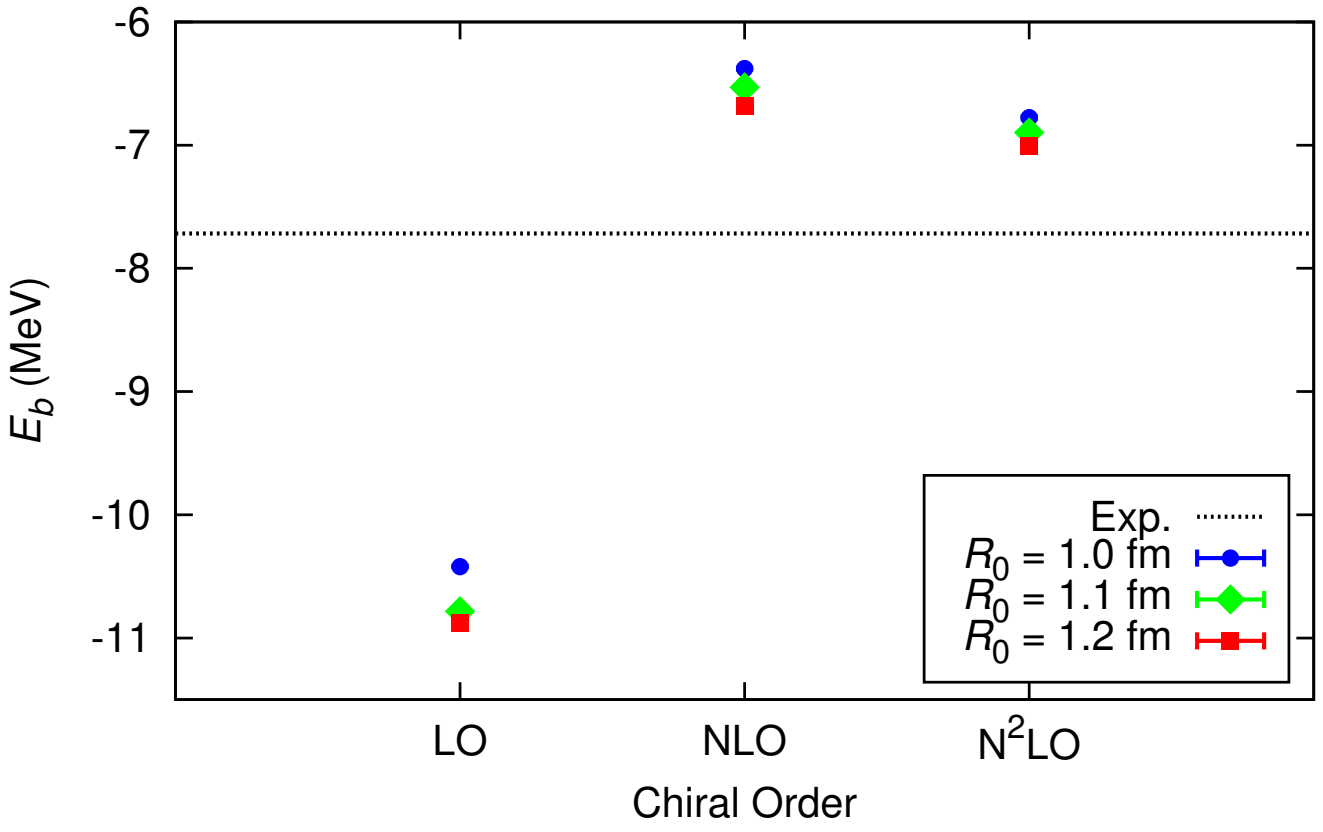

Figure 8: ^{3}He binding energy at different chiral orders and cutoff values.

Results

^{4}He binding energies - $\langle H \rangle$

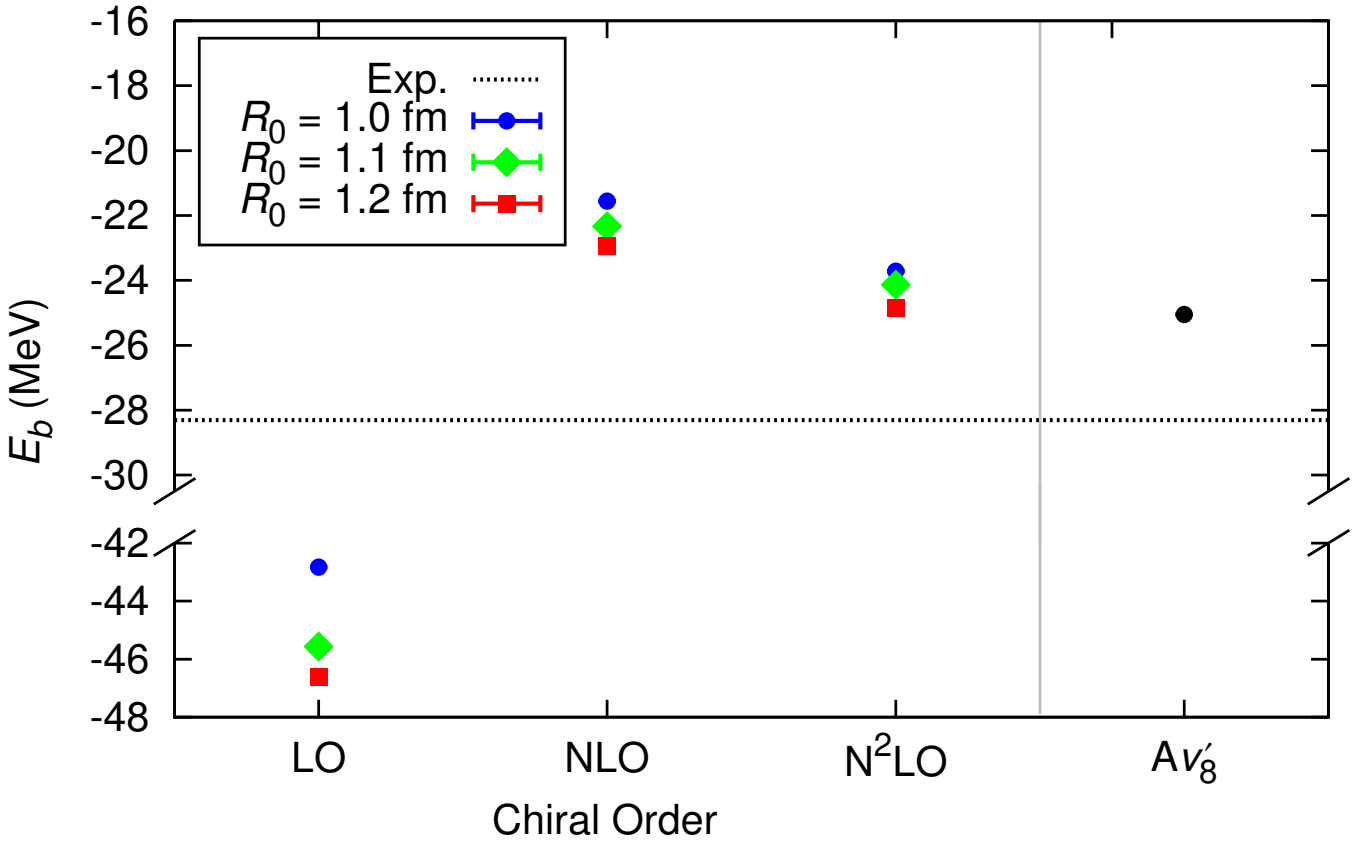

Figure 9: ^{4}He binding energy at different chiral orders and cutoff values.

Results

^{3}H radii - $r^2_{\text{pt.}} = r^2_{\text{ch.}} - r^2_p - \frac{N}{Z} r^2_n$

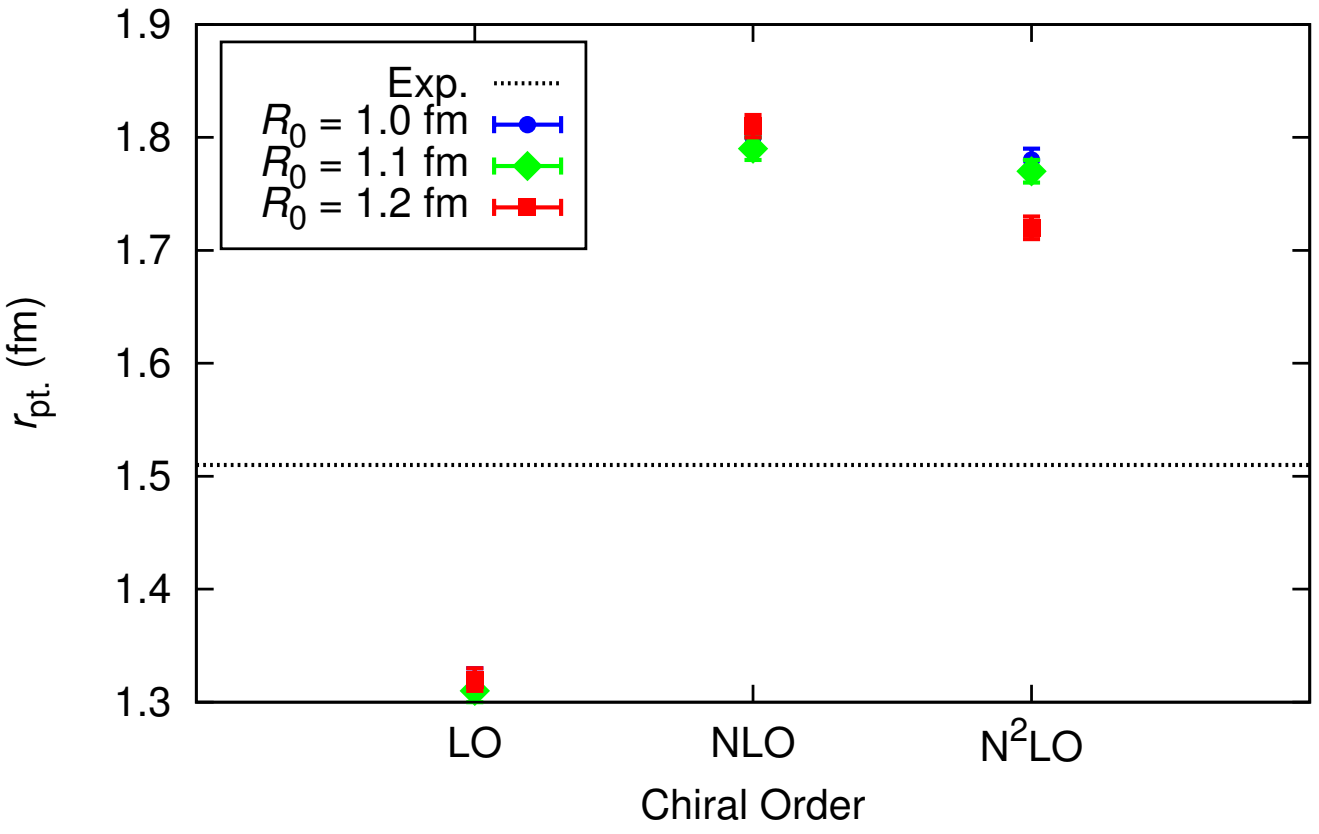

Figure 10: ^{3}H radii at different chiral orders and cutoff values.

Results

^{3}He radii - $r^2_{\text{pt.}} = r^2_{\text{ch.}} - r^2_p - \frac{N}{Z} r^2_n$

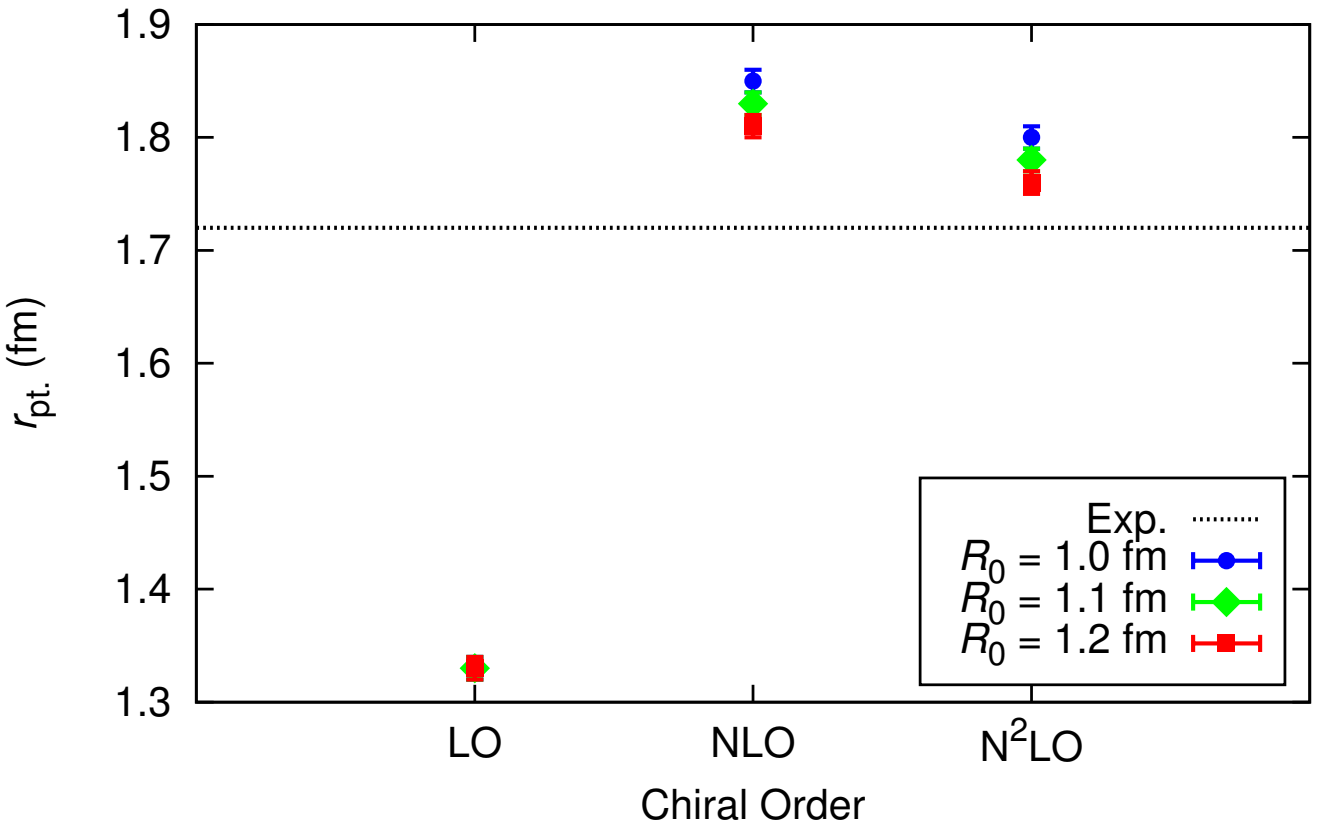

Figure 11: ^{3}He radii at different chiral orders and cutoff values.

Results

^{4}He radii - $r^2_{\text{pt.}} = r^2_{\text{ch.}} - r^2_p - \frac{N}{Z} r^2_n$

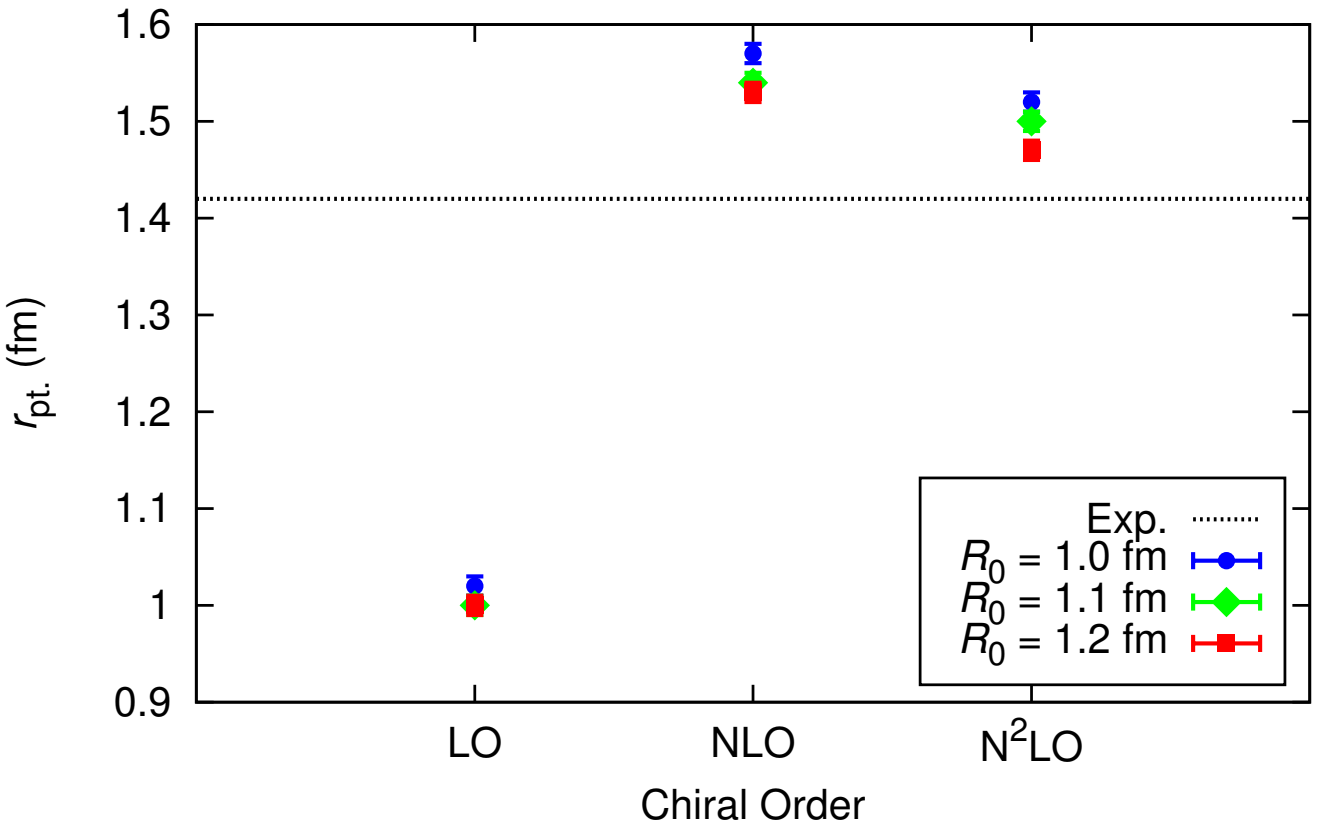

Figure 12: ^{4}He radii at different chiral orders and cutoff values.

Results

^{4}He perturbation - $\langle \Psi_{\mathrm{NLO}} | H_{\mathrm{NLO}} + (V_{\mathrm{N^2LO}} - V_{\mathrm{NLO}}) | \Psi_{\mathrm{NLO}} \rangle$

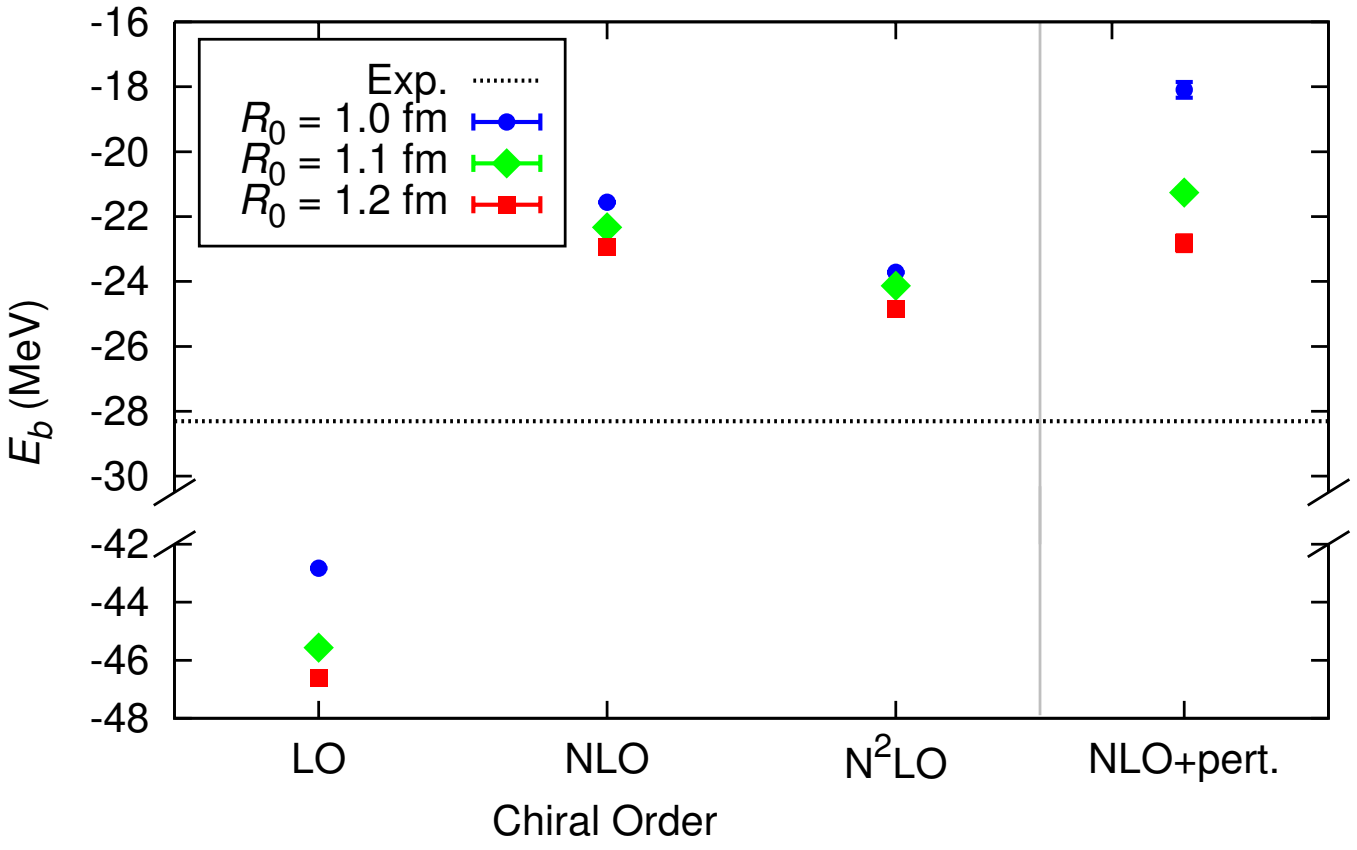

Figure 13: ^{4}He binding energy at different chiral orders and cutoff values plus a first-order perturbative calculation of $\langle H_{\mathrm{N^2LO}} \rangle$.

Results

^{2}H perturbation

Hints from the deuteron.

- Write $H \rightarrow \langle k' J M_J L' S | H | k J M_J L S \rangle$.
- Diagonalize$\rightarrow \{\psi_D^{(i)}(r)\}$.
- Second- and third-order perturbation calculations possible.

Table 1: Perturbation calculations for ^{2}H with different cutoff values for R_0.

Calculation	E_b (MeV)		
	$R_0 = 1.0$ fm	$R_0 = 1.1$ fm	$R_0 = 1.2$ fm
$E^{(0)}_{0\,(\mathrm{NLO})}$	-2.15	-2.16	-2.16
$E^{(0)}_{0\,(\mathrm{NLO})} + V^{(1)}_{\mathrm{pert.}}$	-1.44	-1.80	-1.90
$E^{(0)}_{0\,(\mathrm{NLO})} + V^{(2)}_{\mathrm{pert.}}$	-2.11	-2.17	-2.18
$E^{(0)}_{0\,(\mathrm{NLO})} + V^{(3)}_{\mathrm{pert.}}$	-2.13	-2.18	-2.19
$E^{(0)}_{0\,(\mathrm{N^2LO})}$	-2.21	-2.21	-2.20

Results

Distributions - ^{4}He

Proton distribution: $\rho_{1,p}(r) = \frac{1}{4\pi r^2}\langle\Psi|\sum_i \frac{1+\tau_z(i)}{2}\delta(r-|\mathbf{r}_i-\mathbf{R}_{\rm c.m.}|)|\Psi\rangle$.

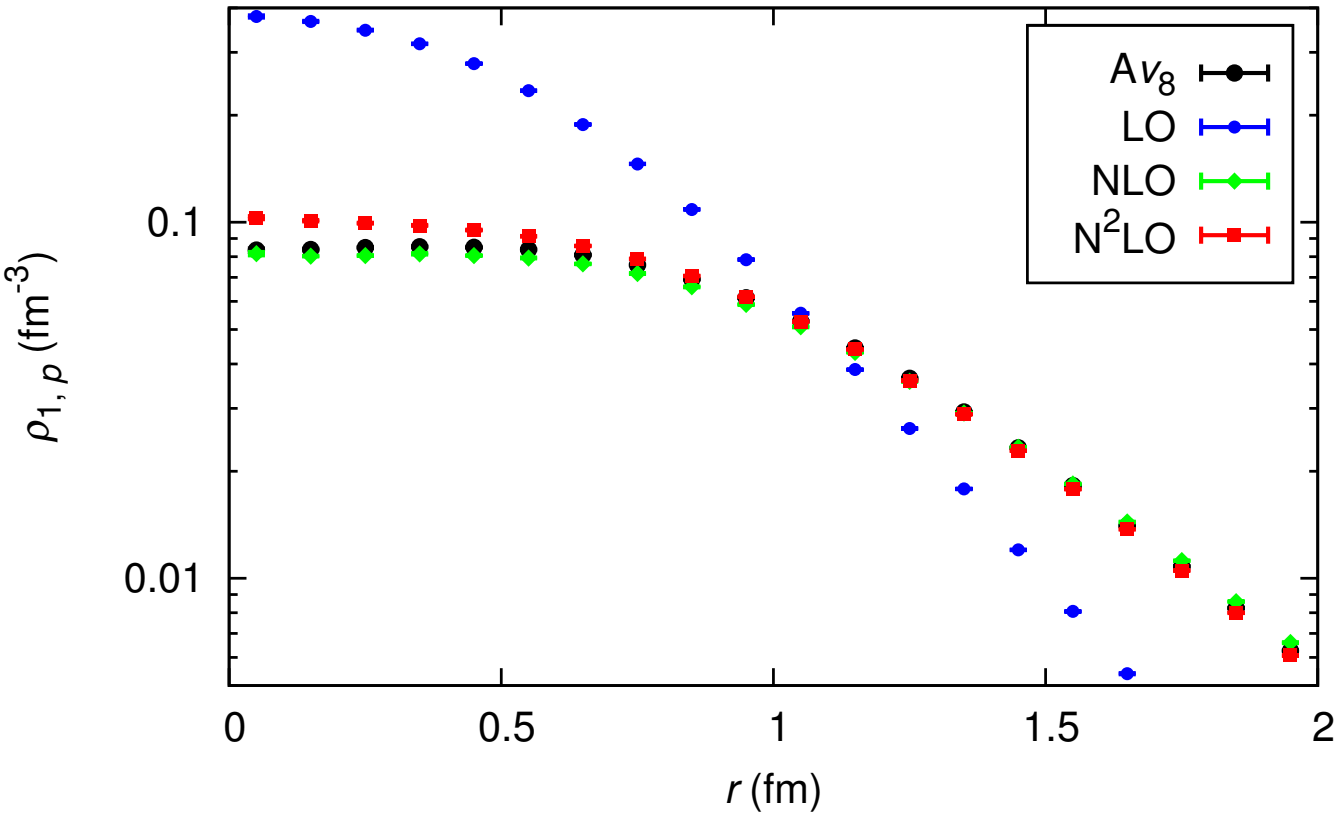

Figure 14: ^{4}He proton distribution at different chiral orders.

Results

Distributions - ^{4}He

Two-body $T = 1$ distribution:

$$\rho_{2,T=1}(r) = \frac{1}{4\pi r^2}\langle\Psi|\sum_{i<j}\frac{3+\boldsymbol{\tau}_i\cdot\boldsymbol{\tau}_j}{4}\delta(r-|\mathbf{r}_{ij}|)|\Psi\rangle.$$

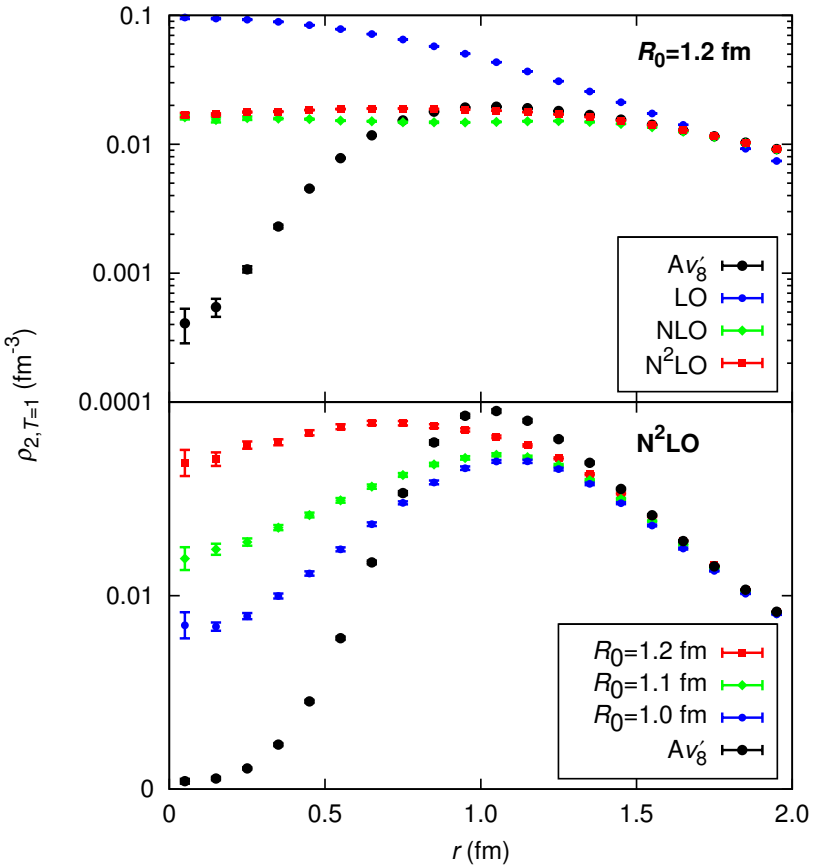

Figure 15: ^{4}He two-body $T = 1$ distributions.

Results

Distributions - ^{4}He

Coulomb Sum Rule: $S_L(q) = 1 + \rho_{LL}(q) - Z|F_L(q)|^2$;
$\rho_{LL}(q) \propto \int d^3 r j_0(qr) \rho_{2,T=1}(r)$.

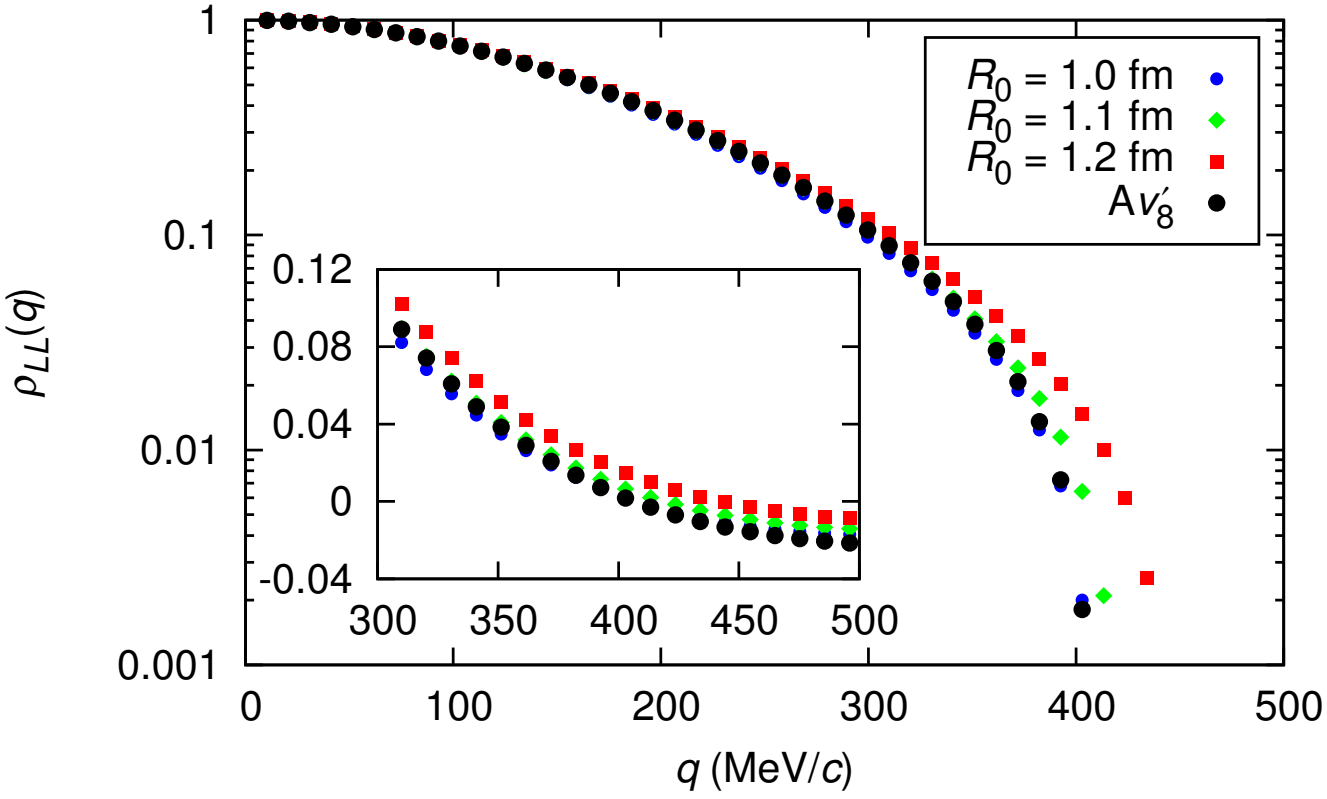

Figure 16: (PRELIMINARY) Fourier transform of the two-body distributions.

Conclusion

Summary

- Nuclear structure calculations probe nuclear Hamiltonians.
  - Phenomenological potentials have been very successful but are perhaps unsatisfactory.
  - Chiral EFT potentials have a more direct connection to QCD, but until now, have been non-local.
- GFMC calculations of light nuclei are now possible with chiral EFT interactions.
- Binding energies at $\mathrm{N^2LO}$ are reasonably similar to results for two-body-only phenomenological potentials.
- Radii show expected trends.
- The softest of the potentials with $R_0 = 1.2$ fm display perturbative behavior in the difference between $\mathrm{N^2LO}$ and NLO.
- The high-momentum (short-range) behavior of chiral EFT interactions is distinct from the phenomenological interactions.

Conclusion

Future work

- Include 3-nucleon force which appears at $\mathrm{N^2LO}$.
- Include 2-nucleon force at $\mathrm{N^3LO}$ (which will be non-local).
- Extend to larger nuclei with $4 < A \leq 12$.
- Second-order perturbation calculation in GFMC.
- Study of, for example, Coulomb sum rule to probe possible consequences of different short-range behavior.

Conclusion

Acknowledgments

Thank you to my collaborators.

- A. Gezerlis
- S. Gandolfi
- J. Carlson
- A. Schwenk
- E. Epelbaum